DESIGN AND PERFORMANCE ANALYSIS OF HYBRID SOLAR POWERED GEYSER IN ISLAMABAD, PAKISTAN

Hassan Elahi[1,2], Ali Tamoor[2,3], Abdul Basit[2], Asif Israr[2], R.F. Swati[2], Shamraiz Ahmad[4], Usman Ghafoor [2], M. Shaban [2]

[1] Department of Mechanical and Aerospace Engineering, Sapienza University of Rome, 00184 Rome, Italy

[2] Department of Mechanical Engineering, Institute of Space Technology, Islamabad, Pakistan

[3] School of Energy and Power Engineering, Xi'an Jiaotaong University, Xi'an, China

[4] Department of Manufacturing & Industrial Engineering, Faculty of Mechanical Engineering, Universiti Teknologi Malaysia, 81310 UTM Johor Bahru, Malaysia

corresponding author: tel: $+393276544166$, email: $hassan.elahi@uniroma1.it$

As a consequence of energy crisis and pollution around the globe, many countries are shifting towards the renewable energy resources which are environmental friendly too i.e., solar energy. The aim of this research work is to design a solar powered geyser that can be used for domestic as well as for industrial purposes. The analytical model is constructed to understand the behavior of water temperature with respect to time and to the energy that can be generated from solar panel with and without glass glazing. The extensive experimentation was carried out at self designed test rig in Islamabad, Pakistan for six months i.e., Aug 2017 - Jan 2018. The response of the power output to the time in specific month and its efficiency is predicted and optimized. Moreover, electrical backup was integrated in closed loop feedback circuit to achieve maximum efficiency even in dark cloudy weather or a sunny day. Moreover, it is calculated that how much external power is required by the system in order to perform the task at different time intervals of the day. Analytical results were in good agreement with experimental results, with error of 9%.

Keywords: Solar, Geyser, Fabrication, Design, Performance, Evaluation, Energy

1 Introduction

Solar based geysers are used for domestic usage where hot water is major thermal demand [1]. The most critical part of the solar geyser is solar collector. The conventional solar geyser operates on the principle that solar collector transform heat to the fluid in tank but it has several disadvantages i.e., performance of heat transfer is low, reverse heat flow and many other problems related to weight and size of the system [2]. Most

of these irregularities can be sort out by using heat pipes in the solar collector to transfer energy. So, by using heat pipes, overall efficiency of the system can be improve [3].

Many researchers have working on mechanisms of clean energy harvesting [4]. One of the most useful mechanism oamong them is to harvest energy using piezoelectric material [5]. Many researchers have analysed there thermal properties and thermal response to voltage generation [6, 7, 8]. The disadvantage of using such materials is that they can harvest energy for micro or nano electronics [9, 10, 11]. Raees et al. presented analytical, experimental and numerical model for these materials [12, 13]. Faisal et al. developed the fatigue analysis and material charcterization for thermal behavior [14].

Latent heat of the fluid is able to transfer energy from one place to another by utilizing heat tubes in a sealed system by evaporation and condensation. The most critical working parameters of the heat tubes are that they should have low temperature gradient and use a small amount of working fluid [15]A lot of research has been done to study the two phase closed thermosiphon (TPCT) behavior and its thermal performance. The thermal performance parameter of TPCT i.e., bending position, working fluid, geometry cross section, fill ratio, heat input and boiling visualization has been of great interest for many researchers [16].

Phase change process is the reason for geyser boiling phenomenon. Boiling occurs in a geyser because of gathered vapor generated in evaporator [17]. The thermosiphon effect works on a fact that density of hot water is less as compared to cold water. So, cold water will move towards solar collector due to higher specific density[18]. The storage tanks of solar geyser systems are mounted over the solar collectors to ensure the thermosiphon principle. When the solar radiations falls onto the solar collector, the water in the tubes of the collector absorbs heat from the radiations and then having lower specific density the hot water in the tubes start moving towards the storage tank of the system [19]. Meanwhile the cold water from the tank reaches down to the solar collector tubes replacing the hot water and in this manner the cycle starts to run in the system. This cycle continues to run till when the equilibrium temperature is achieved [20]. The overhead storage tank of the building has also to play its role in the solar systems. If the overhead tank is not above the storage tank of the solar systems then the thermosiphon effect in the solar system will not be working properly which will hinder the proper working of the solar system [21]. The problem for the solar powered geyser is; due to bad cloudy weather the solar collector is not able to absorb sufficient radiations which results in less energy generation then required [22]. In order to resolve this issue, a hybrid design is needed so that efficiency of the system is not compromised due to uncertain climate conditions [23]

In this research work, a hybrid solar powered geyser is designed and fabricated for clean renewable energy that can be used for domestic as well as for industrial purposes. The analytical calculations are in good agreement with experimental data. Moreover, experimental calculations are also done in order to predict the requirement of average external power needed by the solar powered geyser for backup. This research work is divided in four sections. In section 1, motivation for this project, relevant literature review and introduction is provided. In section 2, analytical calculations are made for designing phase of project. In section 3, experimental campaign is explained. In section 4, results and discussion are demonstrated and finally conclusions are derived.

2 Analytical Phase

Prior to experimentation, analytical model for the desired system is constructed in order to analyze the performance parameters. The analytical phase is basically constituted of designing a hybrid solar powered geyser. The designing phase is further breakdown in to four major categories (i.e., solar panel design, design of geyser, design of backup plan as hybrid and feedback design) which all are interrelated to each other. The overall model of the system is shown in Fig. 1 (d).

2.1 Geyser and Solar Panel Design Parameters

Geyser tanks for water storage are commercially available in different sizes according to the dependency of usage ranging from liters to gallons. The tank is designed in such a way that it should not increase the operational area for the system. By increasing the tank size too much, cost of storage tank will increase and solar collector size will also change depending on the size. The system size should be compact in order for its easy movement and installation. For this research work, 80l capacity tank of length 1m is used for storage. The inner radius of the tank is predicted from Equation 1 [24].

$$V = \pi r_i^2 l \tag{1}$$

Where, V is the volume of tank, r_i is the the inner radius of tank and l is the length of tank. The material of tank was selected to be Galvanized Iron and thickness of GI sheet was selected to be 0.00064m. So, the outer radius r_o of storage tank is calculated to be 0.16014m.

Although, increasing the panel area will increase the working and efficiency of the system, but it will also increase the size and cost of the system. So, the panel size should be economical in size and cost as well. The panel was designed according to following parameters [15].

$$A = lw \tag{2}$$

Where, A is the area of panel, l is the length of panel and w is the width of panel. Calculation of design parameters of panel to decide the desired area for optimum working of system is calculated as [25]:

$$Q_{si} = S_i S_a \eta_d \tag{3}$$

Where, Q_{si} is the Output Heat of the system, S_i is the solar insulation, S_a is the surface area and η_d is the desired efficiency of the system. The output heat calculated is $4387500J$ for the value of solar insulation $937.5Wh/m^2$. Heat per unit time can be defined as [24]:

$$\dot{Q} = \frac{Q_{si}}{T_h} \tag{4}$$

Where, T_h is the heating time and $\dot{Q}$ is the heat per unit time.$\dot{Q}$ is calculated as $1218.75W$. Desired area of the panel can be formulated as:

$$A = \frac{\dot{Q}}{G\alpha\gamma} \tag{5}$$

Table 1 – Solar coefficients [26].

G	$850W/m^2$	T_{in}	$308K$
T_{am}	$308K$	m	$0.01121kg/sec$
U	$8W/m^2K$	t_{ab}	$0.001m$
C_p	$4180J/KgK$	K_w	$0.61W/mk$
ρ_w	$1000kg/m^3$	K_s	$43W/mk$
w	$0.9935m$	τ	0.85
α	0.95	V	$0.080m^3$
D_i	$0.0127m$	D_o	$0.0227m$

Where, G is the incidence radiation, α is the absorption of the point and γ is the irradiation effect. The values of the coefficients are obtained from Table 1.

Area required for the tubes is multiple of the total number of tubes and area of a single tube. In order to, calculate the area of a single tube A_s:

$$A_s = 2\pi r_o^2 + 2\pi r_o h \tag{6}$$

From calculations, area of a single tube is $0.1934m^2$, total number of tubes is 8 and spacing between tubes is 0.10m. Radiation absorbed by the system is given in Table 1 [27] for further details of variables and constant see Ref. [28].

$$Q_F = \acute{F}A[G\alpha\gamma - U(T_FM - T_A)] \tag{7}$$

Where, Q_F is the radiation absorbed by the system and $\acute{F}$ The extra heat losses to plate from fluid. Mean fluid temperature can be formulated as:

$$T_{FM} = \frac{TF_i + TF_o}{2} \tag{8}$$

Where, T_{FM} is the mean fluid temperature and TF_i, TF_o are the inner and outer fluid temperature respectively. The calculated T_{FM} is 315.5K. The extra heat losses from plate to fluid can be formulated as:

$$\acute{F} = \frac{\frac{1}{U}}{W[\frac{1}{(UL(D_o+(W-D_o))F)+(\frac{tab}{\pi}D_oKt)+(\frac{1}{\pi}D_ih_{fi})}]} \tag{9}$$

Where,

$$F = tanh(m\frac{W - D_o}{2}) \tag{10}$$

$$m = \sqrt{\frac{U}{Kt}} \tag{11}$$

Where, U is the overall heat transfer coefficient from absorber plate, K is the thermal conductivity coefficient of absorber plate and t is the thickness of absorber plate. By substituting the values from Table 1 in Equs. 9-11, the value of m is 30.4997 and F is 0.72. The velocity of the fluid can be calculated as:

$$q = \frac{V_{tank}}{Timetofilltank} = V_fA_t \tag{12}$$

So, velocity of the fluid V_f, is calculated as 0.000219 m/s. In order to get Reynold Number Equ. 13 is used and calculated to be 2.76. Nusselt number N_u is calculated from the standard Nusselt table and found to be 5.635 as per calculation by Ravi [29]. So, the radiation absorbed by the fluid is 867.6W and outlet temperature is 326.51K.

$$Re = \frac{\rho V D_i}{\mu} \tag{13}$$

$$h_{fi} = \frac{N_u K f}{Di} \tag{14}$$

Insulation plays a critical role in this phenomenon, in order to measure the parameters for insulation, the heat loss from the storage tank without using the insulation:

$$Q_{noinsulation} = \frac{\Delta T}{\Sigma Rth} \tag{15}$$

Where, $Q_{noinsulation}$ is the heat loss from the storage tank without using the insulation, ΔT is the change in temperature and ΣRth is the summation of thermal resistances. For this designed system thermal resistances are:

$$\Sigma Rth = R_{convective,1} + R_{cylinder} + R_{Convective,2} \tag{16}$$

Where,

$$R_{convective,1} = \frac{1}{h_{water} A_{inlet}} \tag{17}$$

$$R_{cylinder} = \frac{ln\frac{r_o}{r_i}}{2\pi K l} \tag{18}$$

$$R_{convective,2} = \frac{1}{h_{fluid} A_{outlet}} \tag{19}$$

By substituting Equs. 16-19; thermal resistance for convective 1 is $7.4mC/w$, thermal resistance for convective 2 is $49mC/w$, thermal resistance for cylinder is $1356mC/w$ and total thermal resistance is $57.4mC/w$. So, $Q_{noinsulation}$ is 350.0175W.

In order to calculate the heat loss using an insulation, As glass wool insulation was used for insulating the storage tank. So:

$$Q_{ins} = 0.05(Q_{noinsulation}) \tag{20}$$

Where, Q_{ins} is the heat loss using an insulation and calculated to be 17.5W. For this designed system thermal resistances are:

$$\Sigma Rth = R_{convective,1} + R_{cylinder} + R_{insulation} + R_{Convective,2} \tag{21}$$

Where,

$$R_{insulation} = \frac{ln\frac{r_{ins}}{r_o}}{2\pi K_{ins} l} \tag{22}$$

Figure 1 – Experimental setup; (a) Over all test rig, (b) Installation, (c) Mirror glaze, (d) Analytical model, (e) Tubes, (f) Inverter and hybrid system, (g) Control mechanism, (h) Temperature sensor

$$R_{convective,2} = \frac{1}{h_{air} A_{ins}} \tag{23}$$

By substituting Equs. 17, 18, 21-23, ΣRth for insulation is calculated as 1.14 and thickness of insulation is calculated as 0.0508m. This thickness reduces the loss by 95%.

2.2 Hybrid and Feedback Design

In order to improve overall efficiency of the system, a hybrid closed loop programmable circuit for backup is also designed. This circuit is simulated in Proteus Software, LCD is attached in the circuit to get display of inputs and output parameters. In this research work, two inputs are designed i.e., Fluid temperature detection and Water level detection. Tracking of the collector to the sun is designed in correspondence to the setup design by Hua [30]. From the combination of these two inputs four output actions can be performed.

Auto adjusting of the solar panel in order to absorb maximum radiations. If the fluid in the tank is reached to specified temperature then remaining solar energy will be stored in batteries for future usage. If the weather is bad and stored solar energy is finished in batteries then system will be shifted to AC via inverter. If the level of water is low then the minimum level or specified temperature is obtained by fluid in the tank then it will power off the system and vice versa.

3 Experimentation

Extensive experimentation for 6 months i.e., August 2017 to Jan 2018 has been performed in Islamabad, Pakistan and readings are measured on all alternate days. Experimental campaign is shown in Fig. 1. Experimental setup was designed and fabricated to investigate the effect of geyser boiling to performance characteristics[31]. Tracking of the collector to the sun is designed in correspondence to the setup design

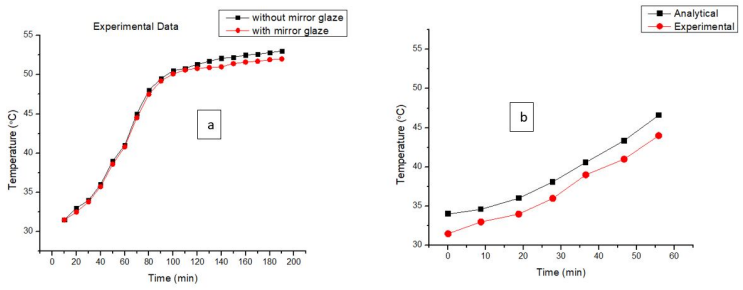

Figure 2 – (a)Response of time vs. fluid average output temp. experimentally.
(b) Response of time vs. fluid average output temp; experimental and numerical comparison.

by Hua [30]. Experimentation was done in five different phases. In Phase 1, analytical results are compared with experimental results for time vs. fluid output temperature. In Phase 2, effect of length and diameter are analyzed with respect to fluid output temperature and its efficiency is analyzed. In Phase 3, Hourly average power is analyzed with respect to time. In Phase 4, Monthly average power is analyzed with respect to months. In Phase 5, efficiency of designed hybrid feedback backup plan is analyzed.

4 Results and Discussion

In phase 1, Fig. 2 (a)represents experimental data to analyze the effect of time from 10 minutes to 190 minutes with respect to output temperature of fluid. Experimentation is performed for solar geyser with and without mirror glaze. It is evident from the graph, the effect of time is a positive linear function up to 90 mins and 45^{o}C of output fluid temperature. After 90 mins of time the temperature tends to be constant for both cases i.e., with and without mirror glazing. The most critical point is 90 mins as after it the difference between mirror glazing and without mirror glazing increases. Fig. 2 (b) represents the analytical data vs. experimental data, the effect of time up to 1 hr is analyzed for the output temperature of fluid. Analytical data is in good agreement with experimental data with error of 8%. These results are in good agreement with work done for Madinah, Saudi Arabia by Benghanem [32].

In phase 2, Fig. 3 (a), the effect of variation in length of the collector absorbing plate from 0.5m to 2.5m is analyzed with respect to output fluid temperature. It is observed that with increasing length, the surface area is increasing and the heat absorbed is also increasing. Length can be varied up to certain limit as after it the cost of system increases; for greater length greater solar panel is needed. From Fig. 3 (a), it was observed that length of a collector plays a vital role in the variation of output fluid temperature. So, in this phase efficiency of the system is analyzed with respect to variation in length of the collector as shown in Fig. 3 (a). It is observed that with increase in the area of collector, the output fluid temperature increases but the overall efficiency of the system decreases. In Fig. 3 (b), the effect of tube diameter ranging from 0.2m to 0.8m is analyzed with respect to output temperature of fluid. It is observed that the variation in dia. of tubes contributes a minimal role for output temperature of the fluid as well as for the overall efficiency of the system.

In phase 3, extensive experimentation has been carried out for six months on alternate days for 12 hours everyday. In Fig. 4, average solar radiation data is collected for six months from Aug 2017 to Jan 2018 from

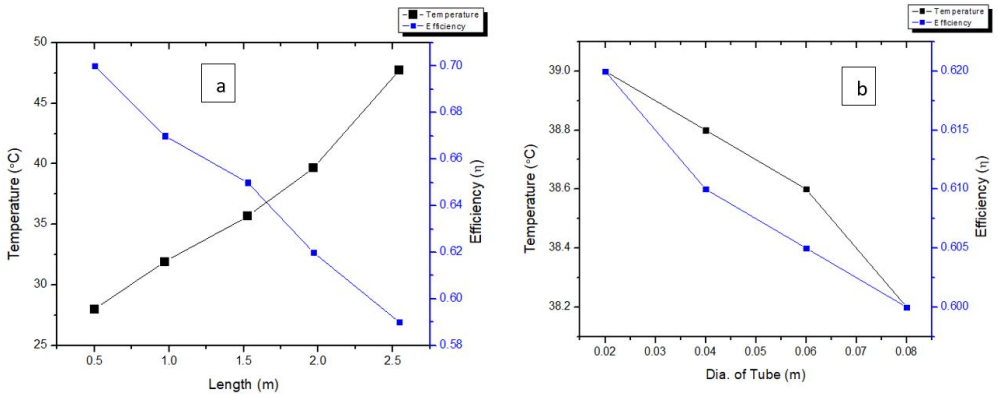

Figure 3 – (a)Effect of length on output temperature of fluid and efficiency of the system. (b) Effect of tube dia. on output temperature of fluid and efficiency of the system.

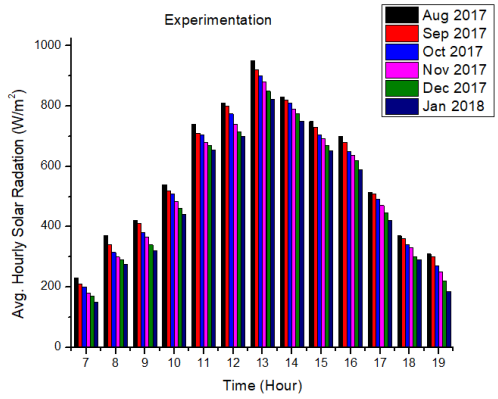

Figure 4 – Bar diagram showing the hourly average global solar radiance for Aug 2017- Jan 2018.

time 07:00 am to 19:00 hours. It is evident from the graph that maximum solar radiation is obtained in the month of August at 13:00 hors in the noon. This result is in good agreement with the work of Bashir [24] for the month of January.

In phase 4, extensive experimentation has been carried out for six months on alternate days for 12 hours everyday. In Fig. 5, average power is collected for six months from Aug 2017 to Jan 2018 from time 07:00 to 19:00 hours. It is evident from the graph that maximum solar radiation is obtained in the month of at 13:00 hors in the noon and minimum at 19:00.

In phase 5, Fig. 6 represents the input power required by the solar system in order to perform the heating of fluid inside the tank. It is observed that on average at the time of 11 am to 3pm no input power is required because at this time rate of irradiation is maximum and maximum input power is required at 19:00 as at this time it has minimum radiation absorption.

5 Conclusion

In this research work, a hybrid solar powered geyser is designed and its performance measurements are analyzed analytically and experimentally at Islamabad, Pakistan for 6 months (Aug 2017 - Jan 2018). Exper-

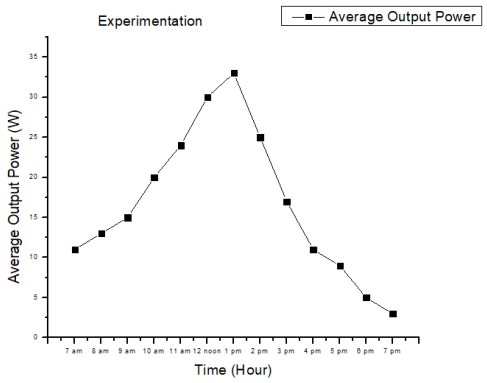

Figure 5 – Avg. output power vs. hours for Aug 2017- Jan 2018.

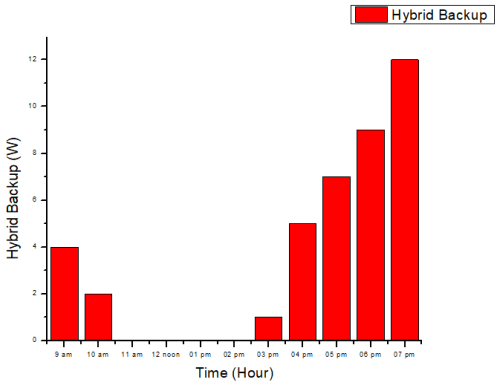

Figure 6 – Avg. input power required from hybrid backup vs. hours for Aug 2017- Jan 2018.

imental results are in good agreement with analytical results with error less than 9%. Following conclusions can be made from this research work. The effect of heating is a linear function up to 90 min. of time, after this effect is constant for output fluid flow. By increasing the length of collector the output fluid temperature increases as more energy can be absorbed but the overall efficiency of the system decreases as the input power requirement of the system also increases with it and the dia. of tubes has minimal effect on efficiency of the system. Maximum solar radiations were absorbed in the month of August at time of 1 pm and minimum in the month of November at time of 7 pm. So, the maximum power that can be obtained from this designed system is 33W. The system is self-sufficient to generate energy from 11 am to 4 pm. After 4 pm external electrical power source is required to perform the desired operation. This system can provide a base for future experimental work and research work as well.

6 Nomenclature

α: Absorption of paint ; A: Absorber plate area; C_p: Specific heat at constant pressure ; D_i: Inner diameter of tubes; D_o: Outer diameter of tubes ; G: Incidence radiation; h: Coefficient of convection heat transfer; t_{ab}: Thickness of sheet; T_{in}: Fluid inlet temperature ; T_{am}: Ambient temperature; U: Overall heat loss coefficient ; V: Storage tank volume

References

[1] Ahmed A Alammar, Raya K Al-Dadah, and Saad M Mahmoud. Effect of inclination angle and fill ratio on geyser boiling phenomena in a two-phase closed thermosiphon–experimental investigation. *Energy Conversion and Management*, 156:150–166, 2018.

[2] Marine Narcy, Stéphane Lips, and Valérie Sartre. Experimental investigation of a confined flat two-phase thermosyphon for electronics cooling. *Experimental Thermal and Fluid Science*, 2018.

[3] Abhishek Saxena and Nitin Agarwal. Performance characteristics of a new hybrid solar cooker with air duct. *Solar Energy*, 159:628–637, 2018.

[4] Hassan Elahi, Marco Eugeni, and Paolo Gaudenzi. A review on mechanisms for piezoelectric-based energy harvesters. *Energies*, 11(7):1850, 2018.

[5] H Elahi, A Israr, RF Swati, HM Khan, and A Tamoor. Stability of piezoelectric material for suspension applications. In *Aerospace Science & Engineering (ICASE), 2017 Fifth International Conference on*, pages 1–5. IEEE, 2017.

[6] Hassan Elahi, Marco Eugeni, Paolo Gaudenzi, Faisal Qayyum, Raees Fida Swati, and Hayat Muhammad Khan. Response of piezoelectric materials on thermomechanical shocking and electrical shocking for aerospace applications. *Microsystem Technologies*, pages 1–8, 2018.

[7] Hassan Elahi, Marco Eugeni, and Paolo Gaudenzi. Electromechanical degradation of piezoelectric patches. In *Analysis and Modelling of Advanced Structures and Smart Systems*, pages 35–44. Springer, 2018.

[8] Zubair Butt, Riffat Asim Pasha, Faisal Qayyum, Zeeshan Anjum, Nasir Ahmad, and Hassan Elahi. Generation of electrical energy using lead zirconate titanate (pzt-5a) piezoelectric material: Analytical, numerical and experimental verifications. *Journal of Mechanical Science and Technology*, 30(8):3553–3558, 2016.

[9] Hassan Elahi, Marco Eugeni, Paolo Gaudenzi, Madiha Gul, and Raees Fida Swati. Piezoelectric thermo electromechanical energy harvester for reconnaissance satellite structure. *Microsystem Technologies*, pages 1–8, 2018.

[10] Zubair Butt, Shafiq Ur Rahman, Riffat Asim Pasha, Shahid Mehmood, Saqlain Abbas, and Hassan Elahi. Characterizing barium titanate piezoelectric material using the finite element method. *Trans Electr Electron Mater*, 18(3):163–168, 2017.

[11] Hassan Elahi, Zubair Butt, Marco Eugnei, Paolo Gaudenzi, and Asif Israr. Effects of variable resistance on smart structures of cubic reconnaissance satellites in various thermal and frequency shocking conditions. *Journal of Mechanical Science and Technology*, 31(9):4151–4157, 2017.

[12] RF Swati, Hassan Elahi, LH Wen, AA Khan, S Shad, and M Rizwan Mughal. Investigation of tensile and in-plane shear properties of carbon fiber reinforced composites with and without piezoelectric patches for micro-crack propagation using extended finite element method. *Microsystem Technologies*, pages 1–10.

[13] RF Swati, LH Wen, Hassan Elahi, AA Khan, and S Shad. Extended finite element method (xfem) analysis of fiber reinforced composites for prediction of micro-crack propagation and delaminations in progressive damage: a review. *Microsystem Technologies*, pages 1–17, 2018.

[14] Faisal Qayyum, Atif Kamran, Asghar Ali, and Masood Shah. 3d numerical simulation of thermal fatigue damage in wedge specimen of aisi h13 tool steel. *Engineering Fracture Mechanics*, 180:240–253, 2017.

[15] David Reay, Ryan McGlen, and Peter Kew. *Heat pipes: theory, design and applications*. Butterworth-Heinemann, 2013.

[16] Thanaphol Sukchana and Naris Pratinthong. A two-phase closed thermosyphon with an adiabatic section using a flexible hose and r-134a filling. *Experimental Thermal and Fluid Science*, 77:317–326, 2016.

[17] TF Lin, WT Lin, YL Tsay, JC Wu, and RJ Shyu. Experimental investigation of geyser boiling in an annular two-phase closed thermosyphon. *International journal of heat and mass transfer*, 38(2):295–307, 1995.

[18] Stephan Scholl. Pillow plate heat exchangers as falling film evaporator or thermosiphon reboiler. In *Innovative Heat Exchangers*, pages 267–294. Springer, 2018.

[19] Anant Shukla, D Buddhi, and RL Sawhney. Solar water heaters with phase change material thermal energy storage medium: a review. *Renewable and Sustainable Energy Reviews*, 13(8):2119–2125, 2009.

[20] Nosa Andrew Ogie, Ikponmwosa Oghogho, and Julius Jesumirewhe. Design and construction of a solar water heater based on the thermosyphon principle. *Journal of Fundamentals of Renewable Energy and Applications*, 3, 2013.

[21] Hainan Zhang, Shuangquan Shao, Yuping Gao, Hongbo Xu, and Changqing Tian. The effect of heating power distribution on the startup time and overshoot of a loop thermosyphon with dual evaporators. *Applied Thermal Engineering*, 2018.

[22] Auroshis Rout, Sudhansu S Sahoo, and Sanju Thomas. Risk modeling of domestic solar water heater using monte carlo simulation for east-coastal region of india. *Energy*, 2018.

[23] Ute B Cappel, Valeria Lanzilotto, Erik MJ Johansson, Tomas Edvinsson, and Håkan Rensmo. X-ray photoelectron spectroscopy for understanding molecular and hybrid solar cells. In *Molecular Devices for Solar Energy Conversion and Storage*, pages 433–476. Springer, 2018.

[24] Muhammad Anser Bashir, Hafiz Muhammad Ali, Shahid Khalil, Muzaffar Ali, and Aysha Maryam Siddiqui. Comparison of performance measurements of photovoltaic modules during winter months in taxila, pakistan. *International Journal of Photoenergy*, 2014, 2014.

[25] Wenfeng Gao, Wenxian Lin, and Enrong Lu. Numerical study on natural convection inside the channel between the flat-plate cover and sine-wave absorber of a cross-corrugated solar air heater. *Energy Conversion and Management*, 41(2):145–151, 2000.

[26] Eduardo I Ortiz-Rivera and Fang Z Peng. Analytical model for a photovoltaic module using the electrical characteristics provided by the manufacturer data sheet. In *Power Electronics Specialists Conference, 2005. PESC'05. IEEE 36th*, pages 2087–2091. IEEE, 2005.

[27] Anil Singh Yadav and JL Bhagoria. A numerical investigation of square sectioned transverse rib roughened solar air heater. *International Journal of Thermal Sciences*, 79:111–131, 2014.

[28] Ambra Giovannelli and Muhammad Anser Bashir. Charge and discharge analyses of a pcm storage system integrated in a high-temperature solar receiver. *Energies*, 10(12):1943, 2017.

[29] Ravi Kant Ravi and RP Saini. Nusselt number and friction factor correlations for forced convective type counter flow solar air heater having discrete multi v shaped and staggered rib roughness on both sides of the absorber plate. *Applied Thermal Engineering*, 129:735–746, 2018.

[30] Chihchiang Hua and Chihming Shen. Comparative study of peak power tracking techniques for solar storage system. In *Applied Power Electronics Conference and Exposition, 1998. APEC'98. Conference Proceedings 1998., Thirteenth Annual*, volume 2, pages 679–685. IEEE, 1998.

[31] Engin Gedik. Experimental investigation of the thermal performance of a two-phase closed thermosyphon at different operating conditions. *Energy and Buildings*, 127:1096–1107, 2016.

[32] M Benghanem. Optimization of tilt angle for solar panel: Case study for madinah, saudi arabia. *Applied Energy*, 88(4):1427–1433, 2011.